Measurement of the branching ratio of $K_L \to e^+e^-\gamma\gamma$

A. Alavi-Harati,[12] T. Alexopoulos,[12] M. Arenton,[11] K. Arisaka,[2] S. Averitte,[10] A. R. Barker,[5] L. Bellantoni,[7] A. Bellavance,[9] J. Belz,[10] R. Ben-David,[7] D. R. Bergman,[10] E. Blucher,[4] G. J. Bock,[7] C. Bown,[4] S. Bright,[4] E. Cheu,[1] S. Childress,[7] R. Coleman,[7] M. D. Corcoran,[9] G. Corti,[11] B. Cox,[11] M. B. Crisler,[7] A. R. Erwin,[12] R. Ford,[7] P. M. Fordyce,[5] A. Glazov,[4] A. Golossanov,[11] G. Graham,[4] J. Graham,[4] K. Hagan,[11] E. Halkiadakis,[10] K. Hanagaki,[8] S. Hidaka,[8] Y. B. Hsiung,[7] V. Jejer,[11] D. A. Jensen,[7] R. Kessler,[4] H. G. E. Kobrak,[3] J. LaDue,[5,*] A. Lath,[10] A. Ledovskoy,[11] P. L. McBride,[7] P. Mikelsons,[5] E. Monnier,[4,†] T. Nakaya,[7] K. S. Nelson,[11] H. Nguyen,[7] V. O'Dell,[7] M. Pang,[7] R. Pordes,[7] V. Prasad,[4] C. Qiao,[4] B. Quinn,[4] E. J. Ramberg,[7] R. E. Ray,[7] A. Roodman,[4] M. Sadamoto,[8] S. Schnetzer,[10] K. Senyo,[8] P. Shanahan,[7] P. S. Shawhan,[4] W. Slater,[2] N. Solomey,[4] S. V. Somalwar,[10] R. L. Stone,[10] I. Suzuki,[8] E. C. Swallow,[4,6] S. A. Taegar,[1] R. J. Tesarek,[10] G. B. Thomson,[10] P. A. Toale,[5] A. Tripathi,[2] R. Tschirhart,[7] Y. W. Wah,[4] J. Wang,[1] H. B. White,[7] J. Whitmore,[7] B. Winstein,[4] R. Winston,[4] T. Yamanaka,[8] and E. D. Zimmerman[4]

(The KTeV Collaboration)

[1]*University of Arizona, Tucson, Arizona 85721*
[2]*University of California at Los Angeles, Los Angeles, California 90095*
[3]*University of California at San Diego, La Jolla, California 92093*
[4]*The Enrico Fermi Institute, The University of Chicago, Chicago, Illinois 60637*
[5]*University of Colorado, Boulder, Colorado 80309*
[6]*Elmhurst College, Elmhurst, Illinois 60126*
[7]*Fermi National Accelerator Laboratory, Batavia, Illinois 60510*
[8]*Osaka University, Toyonaka, Osaka 560 Japan*
[9]*Rice University, Houston, Texas 77005*
[10]*Rutgers University, Piscataway, New Jersey 08855*
[11]*The Department of Physics and Institute of Nuclear and Particle Physics, University of Virginia, Charlottesville, Virginia 22901*
[12]*University of Wisconsin, Madison, Wisconsin 53706*

(Received 23 October 2000; published 30 May 2001)

We report on a study of the decay $K_L \to e^+e^-\gamma\gamma$ carried out as a part of the KTeV/E799 experiment at Fermilab. The 1997 data yielded a sample of 1543 events, including an expected background of 56 ± 8 events. An effective form factor was determined from the observed distribution of the e^+e^- invariant mass. Using this form factor in the calculation of the detector acceptance, the branching ratio was measured to be $\mathcal{B}(K_L \to e^+e^-\gamma\gamma, E^*_\gamma > 5 \text{ MeV}) = (5.84 \pm 0.15 \text{ (stat)} \pm 0.32 \text{ (syst)}) \times 10^{-7}$.

DOI: 10.1103/PhysRevD.64.012003 PACS number(s): 13.20.Eb, 11.30.Er, 13.40.Hq, 14.40.Aq

The process $K_L \to e^+e^-\gamma\gamma$ occurs mainly through kaon Dalitz decay ($K_L \to e^+e^-\gamma$) with an internally radiated photon. As such, measurements of the radiative decay can test radiative correction calculations and probe the form factor of the $K_L\gamma\gamma^*$ vertex. The study of $K_L \to e^+e^-\gamma\gamma$ is also important because it is a significant background to searches for $K_L \to \pi^0 e^+e^-$, a mode which has an important direct CP-violating component and was a primary focus of the KTeV/E799 rare-decay program [1].

The best existing measurements of the branching ratio $\mathcal{B}(K_L \to e^+e^-\gamma\gamma, E^*_\gamma > 5 \text{ MeV})$ were made by the E799-I and NA31 experiments, which measured $(6.5 \pm 1.2 \text{ (stat)} \pm 0.6 \text{ (syst)}) \times 10^{-7}$ [2] and $(8.0 \pm 1.5 \text{ (stat)}^{+1.4}_{-1.2} \text{ (syst)}) \times 10^{-7}$ [3], respectively, based on signals of 58 and 40 events. This paper presents a branching ratio measurement with much higher precision, using data collected by the KTeV/E799 experiment at Fermilab in 1997.

Figure 1 shows a plan view of the KTeV/E799 detector. The Tevatron at Fermilab made an 800 GeV proton beam, typically delivering 3.5×10^{12} protons per minute. The beam was incident on a BeO target. Photons from the target were converted by a lead absorber immediately downstream. Charged particles were then removed with magnetic sweeping. Collimators defined two neutral beams that entered the KTeV/E799 apparatus 94 m downstream of the target. A 65 m vacuum decay region extended to the first drift chamber.

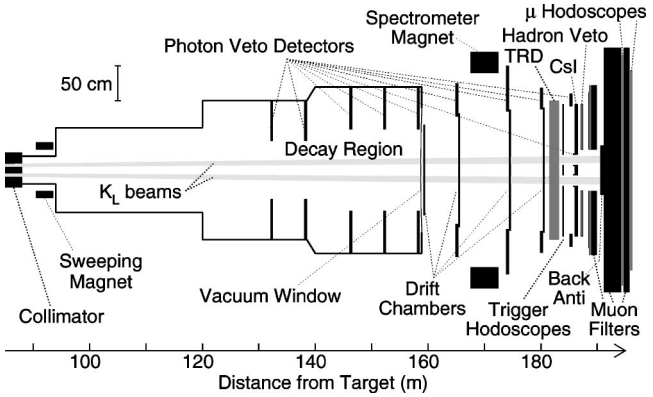

FIG. 1. The KTeV/E799 detector configuration for rare decay studies.

*Corresponding author. Email address: jladue@fnal.gov.
†On leave from C.P.P. Marseille/C.N.R.S., France.

The charged-particle spectrometer consisted of a dipole magnet and four drift chambers (two upstream and two downstream of the magnet) with ~ 100 μm position resolution in both horizontal and vertical directions. The magnetic field imparted a 205 MeV/c horizontal momentum kick. The spectrometer had a momentum resolution of $\sigma(P)/P \sim 0.38\% \oplus 0.016\% P$, where P is in GeV/c.

Photons were detected using an electromagnetic calorimeter, which consisted of 3100 pure CsI crystals, each 50 cm long [4]. Crystals in the central section of the calorimeter had a cross-sectional area of 2.5×2.5 cm^2, and those in the outer region had a 5×5 cm^2 area. The calorimeter's energy resolution for photons was $\sigma(E)/E \sim 0.45\% \oplus 2\%/\sqrt{E}$, where E is in GeV. The position resolution was about 1 mm. By comparing spectrometer momentum to calorimeter energy, $e^{\pm}$ could be distinguished from $\pi^{\pm}$. Nine photon veto assemblies (lead scintillator sandwiches) detected particles leaving the fiducial volume.

Additional $e^{\pm}/\pi^{\pm}$ separation was provided by eight transition radiation detector (TRD) stations located downstream of the last drift chambers [5]. Each TRD station consisted of a polypropylene felt radiator followed by two planes of multiwire proportional chamber (MWPC) filled with an 80/20% mixture of Xe/CO_2 gas. The pulse heights from the 16 MWPC planes, compared with the pion pulse height distributions from a sample of $K_L \to \pi^{\pm} e^{\mp} \nu$ decays, were used to calculate the confidence level that a given track was a pion. Pion rejection factors over 200:1 were possible with a 90% electron efficiency.

The trigger system required hits in two scintillation hodoscopes just upstream of the CsI, as well as drift chamber hits consistent with two coincident charged particles passing through the detector. The trigger used in this study counted the number of isolated clusters of in-time energy over 1 GeV with a special processor [6]; at least four such clusters were required. The total energy deposited in the calorimeter had to be greater than 28 GeV. The scintillator hodoscope behind a lead wall downstream of the calorimeter vetoed events with hadronic showers in the calorimeter, and events with activity in the photon veto system were similarly discarded. Events which passed the hardware trigger requirements were read out into on-line CPUs, which performed basic event reconstruction and applied a few loose event-topology and particle-identification cuts to select events to be written to tape.

During offline event reconstruction, each event was required to contain two tracks from oppositely charged particles originating from a common vertex. The reconstructed vertex had to be between 96 m and 158 m from the target. The tracks had to be at least 1 cm apart at the most upstream drift chamber, with an opening angle between the tracks of at least 2.24 mrad. To select electrons, each track was required to point to a calorimeter cluster with an energy equal, within $\pm 5\%$, to the track momentum measured by the spectrometer. The probability that a track was caused by a pion, formed by combining TRD chamber signals, was required to be less than 4% for each track. The total momentum of all decay products had to be under 216 GeV/c and the total energy greater than 33 GeV. Events with a total of four clusters were analyzed as $K_L \to e^+ e^- \gamma\gamma$ candidates. Events with a total of five clusters were analyzed as $K \to \pi^0 \pi^0_D$ decays, where π^0_D denotes a pion decaying to $e^+ e^- \gamma$. The latter mode was used both to check the simulation and to measure the total number of K_L decays in the data sample.

In addition to the $K_L \to e^+ e^- \gamma\gamma$ signal mode, several potential background processes were considered. The $K_L \to e^+ e^- \gamma$ mode was a background when an additional photon was present. This photon could have been radiated by an $e^{\pm}$ while passing through matter in the detector (''external'' radiation), or it could have been reconstructed from coincidental activity in the calorimeter not associated with the decay (''accidental'' activity). $K \to \pi^0 \pi^0_D$ was a background when one photon was missed. Similarly, $K_L \to \pi^0 \pi^0 \pi^0_D$ could have been a background but was suppressed because missing three photons generally resulted in a reconstructed mass well below the K_L mass. Background from $K_L \to \pi^{\pm} e^{\mp} \nu$ plus two additional accidental photons with the $\pi^{\pm}$ misidentified as $e^{\pm}$ by the calorimeter, was eliminated using the TRDs.

Monte Carlo (MC) simulations of the detector were performed to calculate the acceptances for $K_L \to e^+ e^- \gamma\gamma$ and $K \to \pi^0 \pi^0_D$ and the misidentification rates for $K_L \to e^+ e^- \gamma$, $K \to \pi^0 \pi^0_D$ and $K_L \to \pi^{\pm} e^{\mp} \nu$. The effect of accidental clusters was simulated by overlaying on the MC events with data events taken with a random trigger that had a rate proportional to the beam intensity. The finite angle of external radiation was simulated. Simulations of Dalitz decays included radiative corrections to $\mathcal{O}(\alpha^2_{EM})$ based on the work of Mikaelian and Smith [7]. The radiative correction simulation also quantitatively predicted the ratios $\Gamma(K_L \to e^+ e^- \gamma)/\Gamma(K_L \to \gamma\gamma)$ and $\Gamma(K_L \to e^+ e^- \gamma\gamma)/\Gamma(K_L \to \gamma\gamma)$ and kinematic distributions such as photon energy in the K_L center-of-mass, E^*_γ. The simulations of $K_L \to e^+ e^- \gamma\gamma$ and $K_L \to e^+ e^- \gamma$ used the Bergström, Massó-Singer (BMS) form factor [8]

$$f(x) = \frac{1}{1 - x(m_K^2/m_\rho^2)} + \frac{C\alpha_{K*}}{1 - x(m_K^2/m_{K*}^2)} \times \left[\frac{4}{3} - \frac{1}{(1 - x(m_K^2/m_\rho^2))} - \frac{1}{9(1 - x(m_K^2/m_\omega^2))} - \frac{2}{9(1 - x(m_K^2/m_\phi^2))} \right],$$

where $x = (m_{ee}/m_K)^2$, m_K, m_{K*}, m_ρ, m_ω, and m_ϕ are all invariant masses of corresponding mesons and $C = 2.5$. This includes a parameter α_{K*} describing the relative strengths of the intermediate vector and pseudoscalar meson amplitudes in the $K_L \to \gamma\gamma^*$ vertex.

The number of K_L decays was measured by the $K \to \pi^0 \pi^0_D$ decay mode. This sample was selected with requirements on reconstructed mass and total squared momentum transverse to the K_L flight direction, and had background of $(0.439 \pm 0.044)\%$. Using the acceptance and branching ratio, we determined that there were $(264.2 \pm 1.5$ (stat)

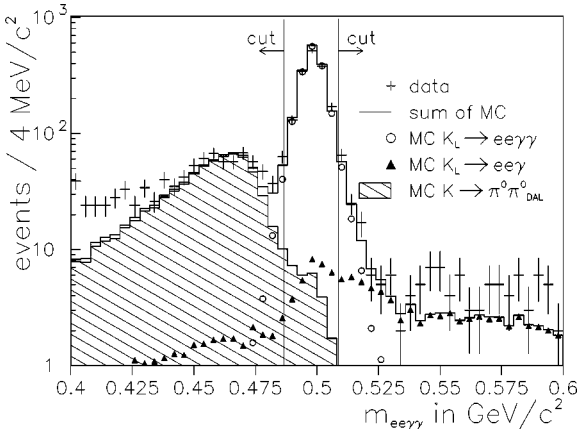

FIG. 2. The $e^+e^-\gamma\gamma$ invariant mass distributions for the data, the $K_L \to e^+e^-\gamma\gamma$ MC, and the background MC samples. The MC distributions use the normalization calculation and predicted branching ratios [for $K_L \to e^+e^-\gamma(\gamma)$] or PDG branching ratio (for $K \to \pi^0\pi^0_D$).

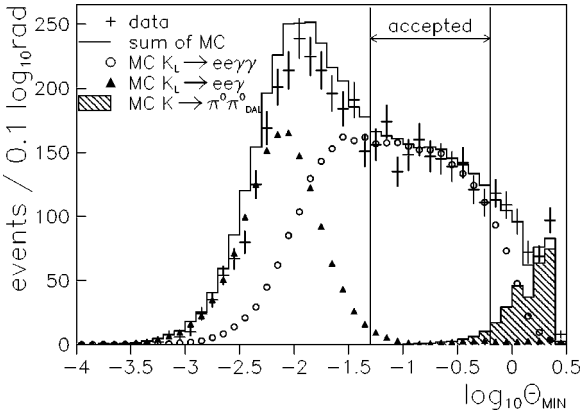

FIG. 3. The $\log_{10}\theta_{min}$ distributions for the data, the $K_L \to e^+e^-\gamma\gamma$ MC, and the background MC samples. The MC distributions use the normalization calculation and predicted branching ratios [for $K_L \to e^+e^-\gamma(\gamma)$] or PDG branching ratio (for $K \to \pi^0\pi^0_D$).

± 2.4 (syst) ± 9.1 (BR)) $\times 10^9$ K_L decays between 20 and 220 GeV/c. The systematic uncertainty only includes effects not common to both signal and normalization mode, and the third uncertainty is due to uncertainties in the branching ratios of $K_L \to \pi^0\pi^0$ and $\pi^0 \to e^+e^-\gamma$ [9].

Several cuts on reconstructed quantities were made on events with exactly four calorimeter clusters to identify $K_L \to e^+e^-\gamma\gamma$ signal candidates. First, to ensure that candidate events did not include radiated photons below the nominal infrared cutoff of 5 MeV, E^*_γ was calculated for each photon and was required to be at least 8 MeV (to allow for finite detector resolution). Since the MC sample was subjected to the same requirement, the acceptance correction procedure yielded a branching ratio valid for $E^*_\gamma > 5$ MeV, allowing direct comparison to theoretical predictions as well as to other published measurements.

In order to reduce backgrounds in which one or more particles are missing or mismeasured in the detector, or which involve accidental activity, a momentum balance cut was imposed. The square of the component of the total momentum of the decay perpendicular to a line drawn from the target to the vertex was required to be less than 300 $(\mathrm{MeV}/c)^2$ for $K_L \to e^+e^-\gamma\gamma$ candidates.

The invariant mass of the decay, $m_{ee\gamma\gamma}$, was calculated assuming that the tracks were electrons. This mass was required to be within 11 MeV/c of the neutral-kaon mass. Figure 2 shows the distributions of $m_{ee\gamma\gamma}$, after all other cuts, for data, signal, and the two main backgrounds. Values of $m_{ee\gamma\gamma}$ for $K \to \pi^0\pi^0_D$ decays tended to be less than the kaon mass because one photon was missing. The excess in data at very low $m_{ee\gamma\gamma}$ was from $K_L \to \pi^0\pi^0\pi^0_D$ decays with three missing photons. The $K_L \to e^+e^-\gamma$ decays often had a mass above the kaon mass because most such decays had an extra, accidental photon. The peak at the kaon mass in the $K_L \to e^+e^-\gamma$ distribution is caused by events with external radiation.

The distributions of minimum angle, θ_{min}, between any photon and any electron in the center of mass of the decay are plotted in Fig. 3 after all other cuts. The small angle events were dominated by $K_L \to e^+e^-\gamma$ with an externally radiated photon. The large angle events were dominated by $K \to \pi^0\pi^0_D$, where the electron directions were relatively uncorrelated with photon directions. Signal events were required to have $0.05 < \theta_{min} < 0.63$ rad.

There were 1,543 $K_L \to e^+e^-\gamma\gamma$ candidate events that satisfied all requirements. The distribution of e^+e^- mass in these events after background subtraction was used to determine the form factor. However, since the MC sample did not include radiative corrections to $K_L \to e^+e^-\gamma\gamma$, an effective parameter, α_{Eff}, was measured rather than the true α_{K*}. We simulated the effect of different effective form factors in the MC simulation by reweighting $K_L \to e^+e^-\gamma\gamma$ and $K_L \to e^+e^-\gamma$ MC events with a ratio of the BMS form factor squared over the generated form factor (where $\alpha_{\mathrm{Eff}} = -0.28$) squared. The χ^2 for data to MC correspondence was found for each of many α_{Eff}. A parabola was fit to the χ^2 as a function of α_{Eff}, and the best fit was found at $\alpha_{\mathrm{Eff}} = +0.016$ with $\chi^2 = 4.3$ for 9 degrees of freedom. Figure 4 shows the ratio of data to MC sample for this value and for $\alpha_{\mathrm{Eff}} = -0.30$.

The statistical uncertainty was found by using 22 subsets of MC events, each the same size as the data. The spread of different α_{Eff} found by using each subset in place of the data was taken as the statistical uncertainty, 0.083. A sample of 12 million $K_L \to \pi^0\pi^0\pi^0_D$ decays was used to check the MC simulation of the acceptance as a function of m_{ee}. A ratio of the data over MC results in a slope of 0.038 ± 0.096 $(\mathrm{GeV}/c^2)^{-1}$ and a $\pm 1\sigma$ range of this slope was fed back into the $K_L \to e^+e^-\gamma\gamma$ simulation, resulting in a systematic uncertainty of ± 0.032 on α_{Eff}. Uncertainty in our ability to reconstruct events with $K_L \to \pi^0\pi^0\pi^0_D$ decays, where the two (usually closely spaced) tracks both passed through one of the beam regions of the first drift chamber led us to assign an uncertainty to α_{Eff} of ± 0.027. Other systematic uncertainties, similar to those assessed below for the branching ratio, were evaluated, but the results were negligible. These systematic uncertainties are combined to give a

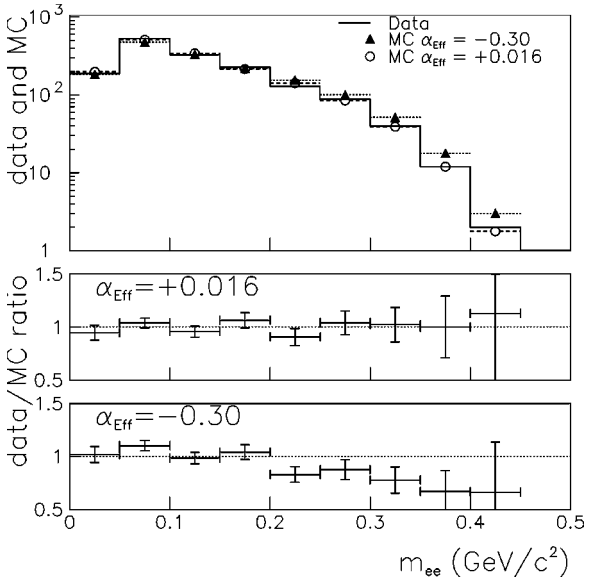

FIG. 4. The raw e^+e^- invariant mass distribution for the data is shown followed by data/MC ratios of e^+e^- invariant mass (m_{ee}) distributions, for MC using $\alpha_{\rm Eff}=0.016$ and $\alpha_{\rm Eff}=-0.30$. The error bars are from data statistics. The MC distributions were normalized to have the same integral as the data distribution.

total uncertainty of ± 0.042 on $\alpha_{\rm Eff}$.

The acceptance for $K_L\to e^+e^-\gamma\gamma$ with generated $E^*_\gamma>5$ MeV was found to be 0.984% using MC calculations reweighted to have $\alpha_{\rm Eff}=+0.016$. A Monte Carlo simulation that was normalized to the number of K_L decays in the detector predicted 31 background events from $K_L\to e^+e^-\gamma$ (and $K_L\to e^+e^-\gamma\gamma$ with true $E^*_\gamma<5$ MeV) and 25 background events from $K\to\pi^0\pi^0_D$. Thus, the branching ratio of $K_L\to e^+e^-\gamma\gamma, E^*_\gamma>5$ MeV is $(5.84\pm 0.15\ (\text{stat}))\times 10^{-7}$.

Several sources of systematic uncertainty for the branching ratio measurement were considered. The normalization calculation contributed uncertainties as mentioned previously. A systematic uncertainty of $\pm 0.49\%$ was assigned in order for the MC to match the relative excess of simulated events at small angles (Fig. 3). Another uncertainty was assigned to account for uncertainty in the inefficiency for tracks in the neutral-beam region of the drift chambers (the beam region was 0.965 ± 0.028 efficient), by reweighting MC events (signal, backgrounds, and normalization) based on the number of tracks in the beam region in each event; the resulting 0.49% drop in branching ratio was taken as a symmetric uncertainty. Varying $\alpha_{\rm Eff}$ by our combined uncertainty of ± 0.093 changed the acceptance and $K_L\to e^+e^-\gamma$ background, and the resulting $\pm 2.25\%$ change in branching ratio was taken as an uncertainty. Finally, uncertainties due to inaccuracies in the MC simulation of the detector were estimated by varying one cut at a time over a reasonable range simultaneously for data, signal, backgrounds, and normalization. The most significant of these uncertainties were from the transverse-momentum cut, the cut on the opening angles between the the two tracks in the lab frame, and the $m_{ee\gamma\gamma}$ cut. When added in quadrature, all of the cut variations contributed a systematic uncertainty of $\pm 3.92\%$. The combined systematic uncertainty on $\mathcal{B}(K_L\to e^+e^-\gamma\gamma, E^*_\gamma>5$ MeV) was $\pm 5.44\%$.

MC numerical integration of the tree-level QED partial width, using the BMS form factor with $\alpha_{K^*}=+0.016$ and $\mathcal{B}(K_L\to\gamma\gamma)=(5.86\pm 0.15)\times 10^{-4}$ [9], predicts $\mathcal{B}(K_L\to e^+e^-\gamma\gamma, E^*_\gamma>5\ \text{MeV})=(5.70\pm 0.14)\times 10^{-7}$, based on $\mathcal{B}(K_L\to e^+e^-\gamma)=(9.1\pm 0.5)\times 10^{-6}$, in agreement with the measurement.

In summary, we have determined the branching ratio of $K_L\to e^+e^-\gamma\gamma$, with an infrared threshold of $E^*_\gamma>5$ MeV, to be $(5.84\pm 0.15\ (\text{stat})\pm 0.32\ (\text{syst}))\times 10^{-7}$. This calculation uses an effective form factor, which does not include effects from radiative corrections, with $\alpha_{\rm Eff}=+0.016\pm 0.083\ (\text{stat})\pm 0.042\ (\text{syst})$. This measurement is an improvement in precision over previous measurements, and agrees with the predicted value at tree level.

We gratefully acknowledge the support and effort of the Fermilab staff and the technical staffs of the participating institutions for their vital contributions. This work was supported in part by the U.S. Department of Energy, The National Science Foundation and The Ministry of Education and Science of Japan.

[1] A. Alavi-Harati *et al.*, Phys. Rev. Lett. **86**, 397 (2001).
[2] T. Nakaya *et al.*, Phys. Rev. Lett. **73**, 2169 (1994).
[3] M.G. Setzu *et al.*, Phys. Lett. B **420**, 205 (1998).
[4] KTeV Collaboration, A. Roodman, in *Calorimetry in High Energy Physics*, Proceedings of the VII International Conference on Calorimetry, Tucson, Arizona, 1997, edited by E. Chev *et al.* (World Scientific, Singapore, 1998).
[5] G. Graham, Ph.D. thesis, University of Chicago, 1999.
[6] C. Bown, E. Cheu, J. Dusatko, H. Sanders and M. Zeleznik, Nucl. Instrum. Methods Phys. Res. A **369**, 248 (1996).
[7] K.O. Mikaelian and J.S. Smith, Phys. Rev. D **5**, 1763 (1972); **5**, 289 (1972).
[8] L. Bergström, E. Massó, and P. Singer, Phys. Lett. **131B**, 229 (1983).
[9] Particle Data Group, D.E. Groom *et al.*, Eur. Phys. J. C **15**, 1 (2000).